

V.M. KADAN,¹ I.Z. INDUTNYI,² V.A. DAN'KO,² P.E. SHEPELYAVYI,²
I.M. DMITRUK,³ P.I. KORENYUK,¹ I.V. BLONSKY¹

¹Institute of Physics, Nat. Acad. of Sci. of Ukraine

(46, Prosp. Nauky, Kyiv 03680, Ukraine; e-mail: kadan@iop.kiev.ua, blon@iop.kiev.ua)

²V.E. Lashkaryov Institute of Semiconductor Physics, Nat. Acad. of Sci. of Ukraine

(41, Prosp. Nauky, Kyiv 03680, Ukraine)

³Taras Shevchenko National University of Kyiv

(2, Academician Glushkov Ave., Kyiv 03127, Ukraine)

INFLUENCE OF TRAP STATES ON THE KINETICS OF LUMINESCENCE AND INDUCED LIGHT ABSORPTION BY Si NANOPARTICLES IN A SiO₂ MATRIX AT THEIR EXCITATION WITH FEMTOSECOND LASER PULSES

PACS 78.67.Bf

We report on the results of our researches dealing with nonlinearities caused by trap states in the lux-intensity characteristics of the intrinsic emission band of Si nanoparticles embedded into a SiO₂ matrix and the dependence of the temporal characteristics of induced absorption on the pump femtosecond pulse fluence.

Keywords: trap states, transient absorption, lux-intensive characteristics, fluence, effect of luminescence fatigue, CCD-camera, Auger-process, pump-probe, white supercontinuum, telegraph-like signal

1. Introduction

The developed surface structure of semiconductor nanoparticles manifests itself in the form of bright anomalies in the photoluminescence (PL) kinetics, for the explanation of which a number of models have been proposed. The “luminescence fatigue” effect, which consists in the time-degradation of the radiation efficiency followed by a saturation (see, e.g., works [1–3]), the formation of photoluminescence radiation in the form of a telegraph-like signal [4, 5], the “charge pump” effect in photoexcited nanoparticles driven by the electron Auger-process promoting the activation capture of photoexcited charge carriers by trap centers in surrounding dielectric SiO_x shells (see, e.g., works [1, 6]), and some others can be regarded as the most known of them. However, all those effects, which continue to be actively studied today in various nano-structured semiconducting substances, are im-

portant for the formation of a long-term (milli- or microseconds) component in the PL quenching kinetics.

In this work, we report on a new feature in the kinetics of photoexcited charge carriers in nano-Si. It corresponds to a picosecond time interval and manifests itself as a superlinear growth of the radiation intensity in the main luminescence band of Si nano-crystals incorporated into a SiO₂ matrix (nano-Si/SiO₂) in the range of excitation intensities, at which the effects of radiation intensity saturation usually take place. In this work, we studied the origin of this anomaly in the luminescence kinetics, as well as the light absorption induced by powerful femtosecond laser pulses.

2. Fabrication of Nano-Si/SiO₂ Specimens

Thin-film SiO_x specimens were obtained by thermally evaporating silicon monoxide (a purity grade of 99.9%, Cerac Inc.) in vacuum at a residual pressure of 2×10^{-3} Pa, following the technology described in work [8]. Polished sapphire wafers arranged at a distance of 25 cm from the evaporator were used as

© V.M. KADAN, I.Z. INDUTNYI, V.A. DAN'KO,
P.E. SHEPELYAVYI, I.M. DMITRUK,
P.I. KORENYUK, I.V. BLONSKYI, 2013

substrates. The deposition rate was 1.6 nm/s. The film thickness was tested *in situ* using the quartz oscillator technique and, after the film deposition, it was measured with the help of a MII-4 microinterferometer. For the examined films, this parameter was equal to 450 nm. After having been deposited, the obtained films were annealed in an argon atmosphere for 15 min at a temperature of 1100 °C. In the course of isothermal annealing, the formation of silicon nanoparticles took place in the oxide matrix of experimental specimens. The corresponding phase separation process in a film SiO_x at high temperatures can be described by the reaction



where $y > x$. The annealing temperature governs the structure of inclusions and the stoichiometry of the oxide matrix after its annealing. Annealing within the limits from 500 to 800 °C leads to a coagulation of Si atoms into amorphous clusters. At annealing temperatures higher than 900 °C, amorphous silicon inclusions crystallize to create Si nano-crystals, the electron structure of which is modified owing to a quantum-mechanical restriction [7]. The structure of the obtained composite layers and their light-emitting properties were studied by the authors of this work with the use of optical, infra-red, and Raman spectroscopies, TEM microscopy, photoluminescence spectrum measurements, and other techniques [8–11]. In particular, it was found that the specimens fabricated under the conditions described above contain silicon nano-crystals about 4 nm in dimension and with a concentration of $5.5 \times 10^{18} \text{ cm}^{-3}$. At an annealing temperature of 1100 °C, SiO_x becomes almost totally decomposed, and the content of the oxide matrix in the obtained specimen is close to SiO_2 ($y \approx 2$).

Other techniques to produce nano-Si ensembles are also known. In particular, these are the implantation of Si ions into a SiO_2 matrix following by the isothermal annealing of specimens [12] and the so-called “wet” (sol-gel) technologies. The advantages of the technology used by us consist in its simplicity, the reproducibility of results, and wide opportunities for the variation of technological regimes.

3. Experimental Part

Non-stationary optical phenomena in nano-Si/ SiO_2 were studied with the use of the “pump-probe” technique developed by us. In this method, laser pulses with a wavelength of 800 nm, a pulse duration of

about 150 fs, and a pulse repetition frequency of 1 kHz were divided into two components with different intensities. One of them was frequency-doubled in a nonlinear LBO crystal (the excitation wavelength was 400 nm, the pulse duration about 200 fs, the excitation spot diameter 0.35 mm, the pulse energy up to 70 μJ , and the average excitation fluence per pulse up to 20 mJ/cm^2); this component was used for the excitation of a specimen normally to the surface. At a fluence of more than 25 mJ/cm^2 , the specimen was destructed. Another component, after having been delayed for a certain femto- to picosecond interval, was focused on a rotating sapphire disk, in which the generation of a “white supercontinuum” with the pulse duration close to 180 fs occurred. In the transmission geometry, the pulses of “white supercontinuum” were focused at a small angle with respect to the exciting beam into the center of a section of the excited specimen and used for reading out the induced variations in absorption. The time dependence of the induced absorption (IA) obtained for researched specimens was scanned by varying the time interval between the excitation and probe pulses. The spectrum of the probe radiation that passed through the excited specimen was registered with the help of an Acton SP500i spectrograph equipped with a CCD-camera. The overall time resolution of this method was close to 400 fs. In review [13], the applied research technique was described in more details.

PL excitation of nano-Si/ SiO_2 for measuring its lux-intensity characteristic integrated over the time does not differ from that described above. The PL spectra were registered at an angle of 45° on an Acton SP500i spectrograph.

4. Experimental Results and Their Discussion

Let us consider the results of measurements obtained for the lux-intensity characteristic, i.e. for the dependence of the total PL intensity (the area S under the spectral curve) on the excitation pulse fluence J . In the inset in Fig. 1, the PL spectra normalized to the same amplitude are plotted for two J -values, 4.3 and 11.5 mJ/cm^2 (making no correction to the spectral sensitivity of the device). One can see that the PL spectrum shape changes little if J varies.

The circles in the main panel of Fig. 1 exhibit the results of measurements for the lux-intensity characteristic $S(J)$. The dependence $S(J)$ has two linear sections with different slopes. At $J > 6 \text{ mJ}/\text{cm}^2$, the slope becomes approximately twice as large pointing

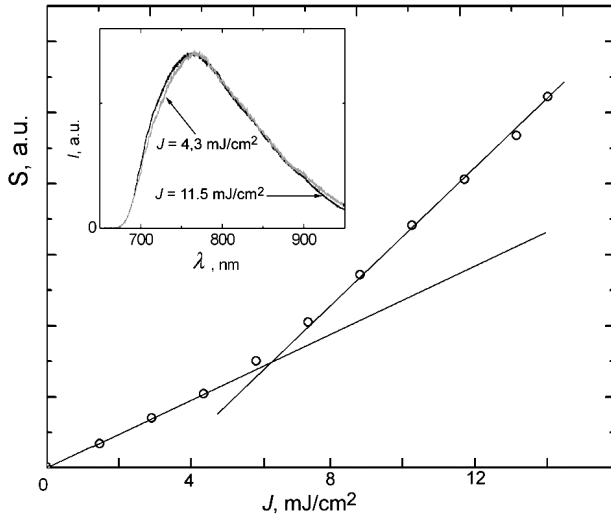


Fig. 1. Lux-intensity characteristic $S(J)$ for nano-Si/SiO₂. The dependence $S(J)$ changes its slope at $J = 6 \text{ mJ}/\text{cm}^2$. In the inset, the normalized PL spectra of nano-Si/SiO₂ at the excitation pulse fluences $J = 4.3$ and $11.5 \text{ mJ}/\text{cm}^2$ are shown

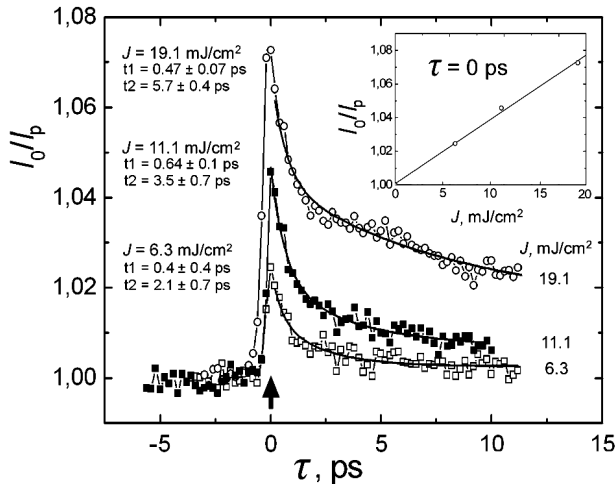


Fig. 2. Dependences of the ratio I_0/I_p on τ at the excitation pulse fluences $J = 6.3, 11.1,$ and $19.1 \text{ mJ}/\text{cm}^2$. In the inset, the dependence of I_0/I_p at $\tau = 0$ on J is shown. The probe light wavelength is 680–690 nm

to a corresponding growth in the quantum yield of luminescence. This growth cannot be explained by the effects of PL radiation stimulation. Really, the stimulation of secondary radiation emission is always accompanied by a variation in the shape of a PL spectrum contour for both uniformly and non-uniformly broadened bands as a result of the selective enhancement of some spectral part. At the same time, as is evident from the insert, an increase of the fluence above the threshold value invokes only minor changes

in the general form of the spectrum. Such a behavior of the lux-intensity characteristic is unexpected, because, when nano-structured silicon is excited with nanosecond laser pulses, the opposite $S(J)$ -behavior is usually observed, which is associated with an enhancement of the role of radiationless Auger recombination at the growth of charge carrier concentration (see, e.g., works [6, 14, 15]). In our opinion, the nonlinear growth of $S(J)$ can be explained by the influence of trap states, which are always present in nano-structures with a developed surface. The peculiarity of femtosecond excitation consists in that, within the time interval that is much shorter than the charge lifetime, the number of generated charge carriers can even exceed the number of available trap states. Then, if we suppose that the number of generated free carriers is still insufficient for filling all trap states at $J < 6 \text{ mJ}/\text{cm}^2$, the latter, by capturing charge carriers, will reduce the PL intensity. The complete saturation of trap states at $J > 6 \text{ mJ}/\text{cm}^2$ gives rise to an increase in the lifetime of free carriers that form the PL radiation either by means of radiative electron-hole recombination or by transforming into radiative states of another nature and, accordingly, to the PL intensity growth.

Moreover, the results obtained provide an opportunity to evaluate the upper limit for the number of trap states per one nanoparticle with an average dimension of 4 nm. The result of our calculations based on the absorption factor measured at a wavelength of 400 nm, $\alpha = 2.7 \mu\text{m}^{-1}$, testifies that a laser pulse with $J = 6 \text{ mJ}/\text{cm}^2$ creates 60 charge carriers, on the average, in a nanoparticle making no allowance for the reflection by nanoparticles and other possible losses. Just this value determines the upper limit for the number of trap states per one nanoparticle. We emphasize that the real number of trap states can be much smaller. For instance, every charge carrier captured through the Auger recombination mechanism is related to a recombination of a $e-h$ pair. In other words, if this mechanism dominates, the presented value should be reduced by a factor of three.

In order to verify our hypothesis concerning the saturation of trap states, we carried out experimental researches of the time-resolved IA in a nano-Si/SiO₂ specimen subjected to the action of femtosecond laser pulses at a wavelength of 400 nm. Following the authors of works [12, 16], we assume that IA emerges as a result of the probe radiation absorption by free charge carriers generated by a femtosecond laser pulse. Of two possible IA mechanisms – absorption by free car-

riers following the Drude mechanism, at which the cross-section grows quadratically as the wavelength increases, and secondary excitation of nonequilibrium charge carriers into higher states – the latter is engaged in the investigated case. This conclusion follows from our measurements of IA at various probe light wavelengths, 680–690 and 610–620 nm, and the same excitation pulse fluence $J = 10 \text{ mJ/cm}^2$. The resistance of the IA signal magnitude to a variation of the probe light wavelength testifies that IA is invoked not following the Drude mechanism, but sooner as a result of the secondary excitation of nonequilibrium charge carriers into higher states. Just this model was used in works [12,16] to explain IA in nano-structured silicon.

In this connection, let us analyze the experimental results depicted in Fig. 2. The IA value was determined as the ratio I_0/I_p between the experimentally measured intensities of probe radiation passed through the non-excited, I_0 , and excited, I_p , specimens. The main panel illustrates the dependences of I_0/I_p on the delay time τ of a probe pulse with respect to the excitation one at various excitation pulse fluences J 's. The experimental results for I_0/I are denoted by hollow squares for $J = 6.3 \text{ mJ/cm}^2$, solid squares for $J = 11.1 \text{ mJ/cm}^2$, and hollow circles for $J = 19.1 \text{ mJ/cm}^2$. In all cases, the ratio I_0/I_p equals 1 if the probe pulse advances the pump one (negative τ -values). The time moment of the excitation is characterized by a drastic increase of IA, with the excitation front growth duration being determined by the installation resolution (about 0.4 ps). After attaining the maximum at $\tau = 0$, the IA magnitude decreases; firstly very quickly, then more slowly. The experimental data for $I_0/I_p(\tau)$ at $\tau > 0$ were approximated by the function $y_0 + A_1 \exp(-\tau/t_1) + A_2 \exp(-\tau/t_2)$ describing a two-exponential decay. The best agreement was achieved for the following values of time constants t_1 and t_2 : for $J = 6.3 \text{ mJ/cm}^2$, $t_1 = 0.4 \pm 0.4 \text{ ps}$ and $t_2 = 2.1 \pm 0.7 \text{ ps}$; for $J = 11.1 \text{ mJ/cm}^2$, $t_1 = 0.64 \pm 0.1 \text{ ps}$ and $t_2 = 3.5 \pm 0.7 \text{ ps}$; and for $J = 19.1 \text{ mJ/cm}^2$, $t_1 = 0.47 \pm 0.07 \text{ ps}$ and $t_2 = 5.7 \pm 0.4 \text{ ps}$.

The inset illustrates the dependence of the IA amplitude at $\tau = 0 \text{ ps}$ (marked by an arrow in the main panel) on J and its linear approximation.

The proximity of the time constant t_1 , which characterizes the initial fall of IA, to the installation time resolution and the linear dependence of the IA magnitude on J testify that the initial peak at $\tau = 0$ is a consequence of the two-photon absorption process,

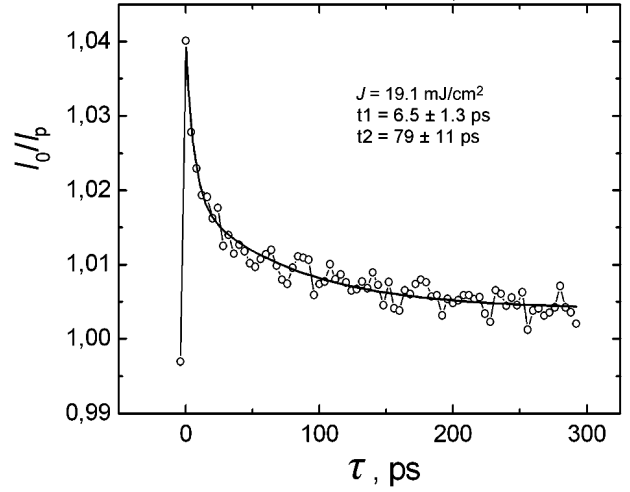


Fig. 3. Long-term dynamics of IA. The excitation pulse fluence $J = 19.1 \text{ mJ/cm}^2$. Two-exponential approximation of the IA reduction is characterized by two time constants, 6.5 and 79 ps

in which one photon from exciting radiation (400 nm, 3.1 eV) and one photon from probe one ($< 690 \text{ nm}$, $> 1.8 \text{ eV}$) participate, because the total energy of those two photons, equal to 4.9 eV, considerably exceeds the direct energy gap width in silicon even if the quantum-size effect is taken into account.

Numerous experimental and theoretical works testify to a high thermalization rate (hundreds of femtoseconds) of “hot” charge carriers, which were generated firstly, onto the bottom of the conduction band in nanocrystalline semiconductors with various compositions (see, e.g., works [17–19]). For this reason, we assume below that the initial thermalization has already terminated within the time interval comparable with the time resolution of the experimental installation, and our subsequent measurements concern the dynamics of thermalized charge carriers.

After the rapid (hundreds of femtoseconds) thermalization of “hot” charge carriers that were generated firstly [17–19], the subsequent fall of IA is characterized by the time constant $t_2 = 2 \div 6 \text{ ps}$, which grows if J increases. By its magnitudes, this constant agrees with the relaxation times obtained in work [16]. Surface Auger recombination is known to be an important mechanism leading to a reduction in the concentration of charge carriers, n_{e-h} , and their lifetime at high excitation levels in nano-structures and thin semiconductor layers (see work [14]). However, as follows from IA measurements, the lifetime t_2 of free carriers, on the contrary, increases if their

concentration grows. In our opinion, such a behavior of t_2 confirms conclusions made earlier concerning the influence of the trap state saturation effect on the dynamics of photoexcited charge carriers. At a relatively low excitation level, the trap centers effectively capture free carriers and diminish their number within a picosecond time interval. If the number of charge carriers generated by an intensive femtosecond excitation pulse exceeds the number of traps, the latter become saturated, which leads to the growth of t_2 . Nevertheless, the given reasoning does not deny the participation of Auger processes in the filling of trap states. The specific mechanism of this filling can be different: both thermally activated transitions into low-energy levels and Auger recombination resulting in the filling of high energy levels. The only important thing is that the both channels of n_{e-h} reduction disappear after all free trap states have been filled.

Hence, the increase in the lifetime of free charge carriers in nano-Si/SiO₂ at the excitation intensity growth is evidenced by both the lux-intensity characteristics (Fig. 1) and the results of IA measurements (Fig. 2). However, the issue concerning the specific mechanism of radiation emission – direct recombination or by means of radiative surface states – remains open. Nevertheless, a conclusion can be drawn that the rapid initial capture of charge carriers occurs onto radiationless states, because it reduces the quantum yield of luminescence at low excitation levels. The cross-section of charge carrier capture by radiationless trap states, which induce a reduction of the luminescence quantum yield, is much larger than that for states forming PL. It is this circumstance that results in a quick (within a few picoseconds) initial reduction in IA until the traps are not filled. After that, as the results of longer-term measurements demonstrate (Fig. 3), IA decreases with time constants of an order of 100 ps. It is this time constant that can characterize the charge carrier transitions into radiative states.

5. Conclusions

Rapid (faster than 10 ps) processes of photoexcited charge carrier capture by trap states are responsible for both their lifetime in the picosecond time range and the quantum yield of luminescence in nano-Si/SiO₂. If the number of charge carriers generated by one femtosecond laser pulse increases, the trap states become totally filled. As a result, the

lifetime of charge carriers substantially grows (to about 80 ps), and the quantum yield of luminescence also does.

The work was partially supported by the State Fund for Fundamental Researches of Ukraine (project F40.2/067), Russian-Ukrainian Program of collaboration development in nanotechnology area in 2012–2013 (project M312), Science and Technology Center in Ukraine (project 5721).

1. I.V. Blonsky, M.S. Brodin, A.Yu. Vakhnin, A.Ya. Zhugaevich, V.N. Kadan, A.K. Kadashchuk, and Yu.G. Pikus, *Mikrosist. Tekhn.* **26**, 224 (2003).
2. D. Kovalev, E. Gross, J. Diener, V. Timoshenko, and M. Fujii, *Phys. Status Solidi C* **2**, 3188 (2005).
3. I.V. Blonsky, M.S. Brodin, A.Yu. Vakhnin, A.Ya. Zhugaevich, V.N. Kadan, and A.K. Kadashchuk, *Fiz. Nizk. Temp.* **28**, 978 (2002).
4. Al.L. Efros and M. Rozen, *Phys. Rev. Lett.* **78**, 1110 (1997).
5. I.S. Osad'ko, *Chem. Phys.* **316**, 99 (2005).
6. I.V. Blonsky, V.M. Kadan, A.K. Kadashchuk, A.Yu. Vakhnin, and A.Ya. Zhugayevych, *Int. J. Nanotechnol.* **3**, 65 (2006).
7. B. Hinds, F. Wang, D. Wolfe, C. Hinkle, and G. Lucovsky, *J. Vac. Sci. Technol. B* **16**, 2171 (1998).
8. V.Ya. Bratus', V.A. Yukhimchuk, L.I. Berezhinskii, M.Ya. Valakh, I.P. Vorona, I.Z. Indutnyi, T.T. Petrenko, P.E. Shepelyavyi, and I.B. Yanchuk, *Fiz. Tekh. Poluprovodn.* **35**, 854 (2001).
9. A. Szekeres, T. Nikolova, A. Paneva, A. Czirakic, Gy.J. Kovacs, I. Lisovskyy, D. Mazunov, I. Indutnyi, and P. Shepeliavyi, *Mater. Sci. Eng. B* **124-125**, 504 (2005).
10. V.A. Dan'ko, I.Z. Indutnyi, V.S. Lysenko, I.Yu. Maidanchuk, V.I. Min'ko, A.N. Nazarov, A.S. Tkachenko, and P.E. Shepelyavyi, *Fiz. Tekh. Poluprovodn.* **39**, 1239 (2005).
11. I.Z. Indutnyi, I.Yu. Maidanchuk, V.I. Min'ko, P.E. Shepelyavyi, and V.A. Dan'ko, *Fiz. Tekh. Poluprovodn.* **41**, 1265 (2007).
12. V.I. Klimov, Ch.J. Schwarz, D.W. McBranch, and C.W. White, *Appl. Phys. Lett.* **73**, 2603 (1998).
13. I.V. Blonsky, I.M. Dmitruk, M.G. Zubrilin, V.M. Kadan, P.I. Korenyuk, I.A. Pavlov, and V.O. Sal'nikov, *Nanosyst. Nanomater. Nanotekhnol.* **6**, 45 (2008).
14. V.A. Zuev, V.G. Litovchenko, and G.A. Sukach, *Fiz. Tekh. Poluprovodn.* **9**, 1641 (1975).

15. I. Mihalcescu, J.C. Vial, A. Bsiesy, F. Muller, R. Romestain, E. Martin, C. Delerue, M. Lannoo, and G. Allan, *Phys. Rev. B* **51**, 17605 (1995).
16. A. Othonos, E. Lioudakis, and A.G. Nassiopoulou, *Nanoscale Res. Lett.* **3**, 315 (2008).
17. J.Z. Zhang, *J. Phys. Chem B*, **104**, 7239 (2000).
18. A.L. Stroyuk, A.I. Kryukov, S.Ya. Kuchmii, and V.D. Pokhodenko, *Teor. Eksp. Khim.* **41**, 67 (2005).
19. S.V. Gaponenko, *Optical Properties of Semiconductor Nanocrystals* (Cambridge University Press, Cambridge, 1996).

Received 11.05.12.

Translated from Ukrainian by O.I. Voitenko

В.М. Кадан, І.З. Індутний, В.А. Данько, П.Є. Шепелявий, І.М. Дмитрук, П.І. Коренюк, І.В. Блонський

ВПЛИВ ПАСТКОВИХ СТАНІВ НА КІНЕТИКУ ЛЮМІНЕСЦЕНЦІЇ ТА НАВЕДЕНОГО ПОГЛИНАННЯ СВІТЛА НАНОЧАСТИНКАМИ Si В SiO₂ МАТРИЦІ ПРИ ЗБУДЖЕННІ ФЕМТОСЕКУНДНИМИ ЛАЗЕРНИМИ ІМПУЛЬСАМИ

Резюме

Розглянуто нелінійності люкс-інтенсивності характеристики власної смуги випромінювання наночастинок Si, інкорпорованих в SiO₂ матрицю, і залежність часових параметрів наведеного поглинання від густини енергії збуджуючого фемтосекундного імпульсу, які зумовлені дією пасткових станів.